

RESPONSES OF TURBULENT CHANNEL FLOWS TO TEMPORAL ACCELERATION

Seo Yoon Jung

Korea Atomic Energy Research Institute
Daejeon 34057, Republic of Korea
syjung77@kaeri.re.kr

Kyoungyoun Kim

Department of Mechanical Engineering
Hanbat National University
Daejeon 34158, Republic of Korea
kkim@hanbat.ac.kr

ABSTRACT

The effects of mean flow acceleration on near-wall turbulent structures were investigated by performing direct numerical simulations of transient turbulent flows in a channel. The simulations were initiated with a fully developed turbulent channel flow and then temporal accelerations were applied. During the acceleration, almost linearly increasing excursions of the flow rate were imposed between the steady initial and final values. The initial Reynolds number (based on the friction velocity) was fixed to $Re_{\tau,i} = 180$, and four different final Reynolds numbers ($Re_{\tau,f} = 250, 300, 350$, and 395) were selected to show the effects of the Reynolds number ratio ($Re_{\tau,f}/Re_{\tau,i}$) on the transient channel flows. To elucidate the effects of the flow acceleration rates on the near-wall turbulence, a wide range of acceleration durations has been examined. Various turbulent statistics and instantaneous flow fields revealed that the rapid increase in the flow rate invokes bypass-transition-like phenomena in the transient flow. In contrast, the flow evolves progressively and the transition does not occur clearly for the mild flow acceleration. When the increase in the Reynolds number is small during the acceleration, distinct bypass-like transition phenomena do not appear in the transient flows, regardless of the acceleration rate. The present study proposed new criteria based on the impulse of the acceleration in order to explain the transition to the new turbulence in the transient channel flow. The bypass-like transition is primarily due to the larger contribution of the impulse to the increase in the flow rate compared with that in viscous friction.

INTRODUCTION

Transient turbulent flow inside a channel is an unsteady flow generated by temporal changes of the pressure gradient or the flow rate. The transient turbulent channel flows can be encountered in many engineering problems, such as the intake of an engine, heat exchangers, valves, or the starting and stopping operations of power plants. Numerous experimental and numerical studies on the transient turbulent channel flows have been conducted; however, intriguing characteristics of transient flows still remain not fully understood. For instance, the response mechanism of the near-wall turbulence to temporal acceleration is still an open question in fundamental turbulence research. In addition, the conventional turbulence models that are widely applied in engineering cannot yet accurately predict the transient flow in a turbulent channel.

Kataoka *et al.* (1975) used an electrochemical method to measure the changes in the flow when the flow rate changes inside a pipe. They found that the time for the transition from laminar to turbulent state decreases with increasing Reynolds number. Mizushima *et al.* (1975) observed a time delay in the response of turbulence, i.e., which reacts to an abrupt change of flow rate slower than the mean flow field, in the transient flow inside a pipe when triggered by a sudden increase of flow rate in the steady state. The delay is more prominent in the center of the pipe than close to the wall. He & Jackson (2000) examined the temporal changes in transient flows,

when the flow is either accelerated or decelerated, utilizing the laser Doppler velocimetry (LDV). They observed three delays in the turbulence: a delay in the turbulence production, a delay in turbulence energy redistribution, and a delay in the propagation of turbulence toward the radial direction. Greenblatt & Moss (2004) conducted experiments of transient pipe flows to examine the effects of flow rate which was higher than those considered in the previous studies (Mizushima *et al.*, 1975; He & Jackson, 2000). The authors identified the regimes of the transient flow as the steady, initial, and final states. They also identified the reconstitution of the wake in the final phase.

Due to the rapid development of supercomputers, numerical studies regarding the transient flow are becoming more popular. Jung & Chung (2012) examined the temporally accelerated flow in the pipe using large-eddy simulation (LES). They numerically confirmed the three delays in the propagation of turbulence in the radial direction, the turbulence production and the redistribution of the turbulence energy, as pointed out in the experiment He & Jackson (2000). In addition, Jung & Chung (2012) analyzed the conditionally averaged flow fields associated with Reynolds shear stress producing events. They showed that sweeps and ejections were closely linked to the delays of the turbulence production and of turbulence propagation away from the wall. He & Seddighi (2013) claimed, through the direct numerical simulation (DNS) study on the transient turbulent channel flow, that the abrupt increase of the flow rate causes similar phenomena to the bypass transitions observed in the laminar boundary layer even though the initial flow is turbulent. They explained that the initial turbulence prior to the acceleration acts as a disturbance to create elongated streaks close to the wall, and then these streaky structures are exposed to secondary instabilities which generate a bundle of turbulence vortices, i.e., turbulent spots. In their subsequent study (He & Seddighi, 2015), it was found that, as the difference between the initial and final Reynolds number increases, the bypass-like transition phenomena becomes more prominent while they becomes uncertain as the Reynolds number difference decreases. It has also been reported that a pipe flow following a step increase in flow rate exhibits the transition which is effectively a laminar-turbulent transition, similar to channel flow (He *et al.*, 2016).

Several parameters have been proposed to characterize the transient turbulent flows. He & Jackson (2000) suggested that factors such as the initial Reynolds number, final Reynolds number, and various dimensionless ramp rate parameters define the transient flows inside pipes. The initial and final Reynolds numbers determine the initial and later states of the transient flows, respectively, while the flow increase rate is associated with the difference in the transient flow from the steady flow corresponding to the same Reynolds number. He & Seddighi (2015) claimed that the difference between the initial and final Reynolds numbers determines the occurrence of the bypass-like transition. They showed that in the case of rapid acceleration, a laminar flow similar to Stokes first

problem appears at the early stage of transient flow and then develops into a final turbulent state. When the final Reynolds number is high, the development of the flow is similar to a bypass-like transition. On the other hand, if the final Reynolds number is low, the flow progressively evolves to the final turbulent state, which exhibits similar transient flow response characterized by the laminar-turbulent transition (He & Seddighi, 2015). However, one can argue that even if the difference is significant, the transition might not occur when the flow rate increases very slowly. Seddighi *et al.* (2014) have investigated effects of a mild acceleration and compared the results with those of rapid acceleration of He & Seddighi (2013). However, it should be noted that the test cases of Seddighi *et al.* (2014) are limited to the range of rapid acceleration rates that cause bypass-like transitions.

In this work, we have performed a series of spectral DNS of the turbulent channel flow with temporal acceleration by the prescribed time-dependent mean pressure gradient to examine the flow parameters relevant to the transition behavior. The initial Reynolds number based on the friction velocity was fixed to $Re_{\tau,i} = 180$ and four different final Reynolds numbers ($Re_{\tau,f} = 250, 300, 350,$ and 395) were selected to show the effects of the Reynolds number ratio ($Re_{\tau,f}/Re_{\tau,i}$) on the transient channel flows. The acceleration time is defined as $T^* = Tu_{\tau,i}/h$, where $u_{\tau,i}$ is the initial friction velocity and h is the half-height of the channel. A wide range of acceleration times has been tested to investigate the effects of the flow acceleration rates on the near-wall turbulence. The main emphasis of the present study is placed on the criteria on the occurrence of the bypass-like transition in temporally accelerating channel flows. A new criteria has been proposed on the basis of the impulse of the acceleration in order to explain the transition to the new turbulence in the transient channel flow. The bypass-like transition is primarily due to the larger contribution of the impulse to the increase in the flow rate compared with that in viscous friction.

COMPUTATIONAL DETAILS

The non-dimensional governing equations of an unsteady, incompressible flow are

$$\frac{D\mathbf{u}}{Dt} = -\nabla p + \frac{1}{Re_{\tau,i}} \nabla^2 \mathbf{u} + \left(-\frac{\partial \langle p \rangle}{\partial x}(t) \right) \mathbf{e}_x \quad (1)$$

$$\nabla \cdot \mathbf{u} = 0 \quad (2)$$

where \mathbf{u} is the velocity and p is the pressure. Here, all variables are non-dimensionalized by the channel half-height h , and the initial frictional velocity $u_{\tau,i}$. The Reynolds number is defined as $Re_{\tau,i} = u_{\tau,i}h/\nu$, where ν is the kinematic viscosity. The last term on the right-hand side of Eq. (1) denotes the mean pressure gradient related to the flow acceleration. The mean pressure gradient is 1.0 in the statistically steady flow. However, in the accelerated flow, the mean pressure gradient increases to a value greater than unity. To generate a linear increase of the flow rate during an acceleration period, a time-dependent mean pressure gradient was imposed in Eq. (1). By integrating the ensemble-averaged streamwise momentum equation over a cross-section of the channel, the time-dependent mean pressure gradient can be written as

$$-\frac{\partial \langle p \rangle}{\partial x}(t) = \frac{1}{2Re_{\tau,i}} \frac{dRe_m}{dt} + \left(\frac{Re_{\tau}(t)}{Re_{\tau,i}} \right)^2 \quad (3)$$

Here, Re_m is the bulk mean Reynolds number ($Re_m = U_m 2h/\nu$). In Eq. (3), the first term on the right-hand side contributes to the

increase in the flow rate, while the second term contributes to the increase in the skin friction when the flow is accelerated by the time-dependent mean pressure gradient. The second term on the right-hand side of Eq. (3) requires the variations in the friction velocity with time, which is unknown. In the present study, $Re_{\tau}(t)$ is computed using the empirical relationship ($c_f = 0.073Re_m^{-0.25}$) by Dean (1978) with an assumption of quasi-steady state conditions during the acceleration period. Time integration of the governing equations is achieved by a semi-implicit method where the implicit Crank-Nicolson scheme is used for the viscous terms and the explicit Adams-Bashforth scheme is employed for the nonlinear convective terms. The spatial derivatives are obtained by using a spectral method with Fourier representations in the streamwise and spanwise directions, and Chebyshev expansion in the wall-normal direction. Periodic boundary conditions are applied in the streamwise and spanwise directions, and the no-slip boundary condition is imposed on the velocity at the solid walls. More details on the numerical method are given in Kim *et al.* (2008). The domain size is $(L_x, L_y, L_z) = (4\pi h, 2h, \pi h)$ in the streamwise, wall normal, and spanwise directions, respectively, which is sufficiently large in comparison with other DNS studies. The grid used is $(N_x, N_y, N_z) = (257, 129, 129)$. The computational domain size and grid resolution are $(L_x^+, L_z^+) = (2262, 565)$, $(\Delta x^+, \Delta z^+) = (8.84, 4.42)$, and $(L_x^+, L_z^+) = (4964, 1241)$, $(\Delta x^+, \Delta z^+) = (19.39, 9.69)$ in wall units corresponding to the initial Reynolds number $Re_{\tau,i} = 180$, and final Reynolds number $Re_{\tau,f} = 395$, respectively. For every test case, four independent simulations are performed to calculate the ensemble-averaged quantities.

RESULTS AND DISCUSSION

Figures 1(a) and 1(b) show the imposed mean pressure gradient and temporal variation of the bulk mean Reynolds number for $Re_{\tau,f} = 395$. Simulations were conducted for five different values of acceleration time ($T^* = 0.1, 1.0, 3.0, 5.0$ and 10.0). In Fig. 1(a), significant changes in the mean pressure gradient are clearly seen as the duration of acceleration becomes shorter. This is due to the rapid increase of the flow rate as shown in Fig. 1(b), which results in a significant increase in the first term on the right-hand side of Eq. (3). After the acceleration period, the mean pressure gradient is imposed as a constant value corresponding to the steady flow at $Re_{\tau,f}$. In Fig. 1(b), for $T^* = 0.1$, a nonlinear increase in the bulk mean Reynolds number is observed, which is due to the use of Dean's correlation for calculating the friction velocity in Eq. (3). In the case of small T^* , the relationship between Re_m and c_f during acceleration is significantly different from Dean's correlation. However, when T^* is small, dRe_m/dt on the right-hand side of Eq. (3) becomes dominant whereas the influence of $(Re_{\tau}/Re_{\tau,i})^2$ on the total mean pressure gradient is meager. He & Jackson (2000) also reported that dRe_m/dt provides a dominant contribution to the mean pressure gradient in the pipe flow with a strong acceleration. This can be confirmed from Fig. 1(c) which shows that the temporal variation in c_f of the present study, imposing the mean pressure gradient with Dean's correlation, is very similar to that of He & Seddighi (2013) where the exact linear increase in the mean flow rate was imposed.

Figures 2(a) and 2(b) show the evolution of the vortical structures for $T^* = 0.1$ and $T^* = 5.0$, respectively. The vortices are visualized using iso-surfaces of the swirling strength (Chakraborty *et al.*, 2005). For $T^* = 0.1$ (Fig. 2a), it was found that the turbulence structures are sparsely distributed at $t^* = 0.4$ after the acceleration. At $t^* = 0.6$, vortex packets occur, wherein the turbulent structures cluster locally. These structures are further developed with increasing time until the entire wall is covered with vortical structures. This is consistent with the results obtained by He &

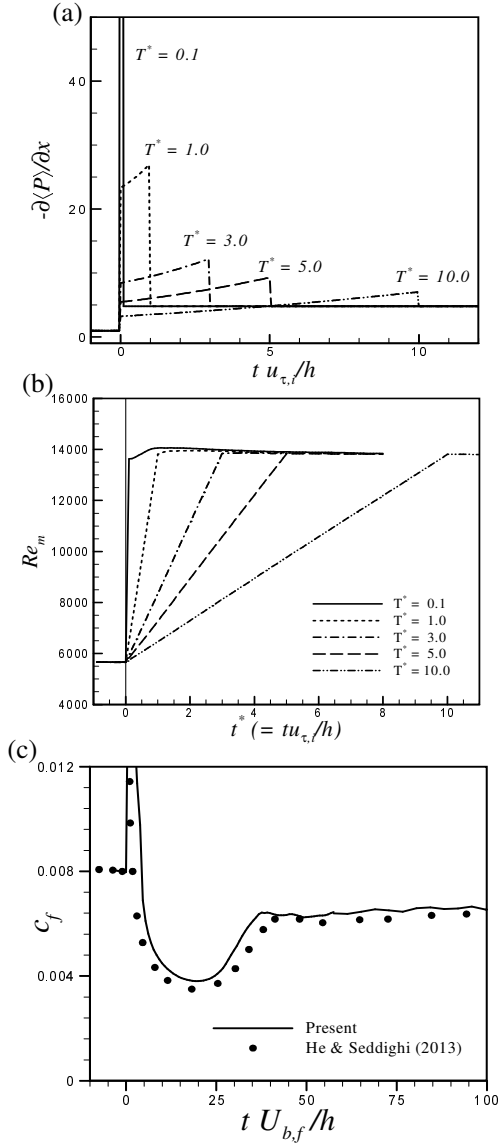


Figure 1. (a) Prescribed mean pressure gradient given by Eq. 3; (b) Development of bulk mean Reynolds number for $Re_{\tau,f} = 395$; (c) Comparison of skin friction coefficient development for different flow accelerating methods. The prescribed mean pressure gradient increase (present, $T^* = 0.1$) and the prescribed mass flow rate increase (He & Seddighi (2013), $T^* = 0.0053$) are shown.

Seddighi (2013). They reported that, following a rapid increase in the flow rate, the turbulent channel flow undergoes a transition that is strikingly similar to the bypass transition in a boundary layer subject to free-stream turbulence. On the other hand, for $T^* = 5.0$ (Fig. 2b), the development of the transient turbulent flow is progressive from the initial state to the final one. The instantaneous pictures represent that, even if the Reynolds number ratio ($Re_{\tau,f}/Re_{\tau,i}$) is high, the transition does not occur in the case of the long duration of acceleration.

Figure 3(a) displays the temporal changes in the skin friction coefficient for various acceleration times in the case of $Re_{\tau,f} = 395$. When the acceleration time is short ($T^* = 0.1$ and 1.0), a sudden increase in c_f is observed in the initial stage of acceleration. This happens because a large pressure gradient is applied abruptly. After the abrupt increase of c_f , a rapid decrease of the coefficient can be

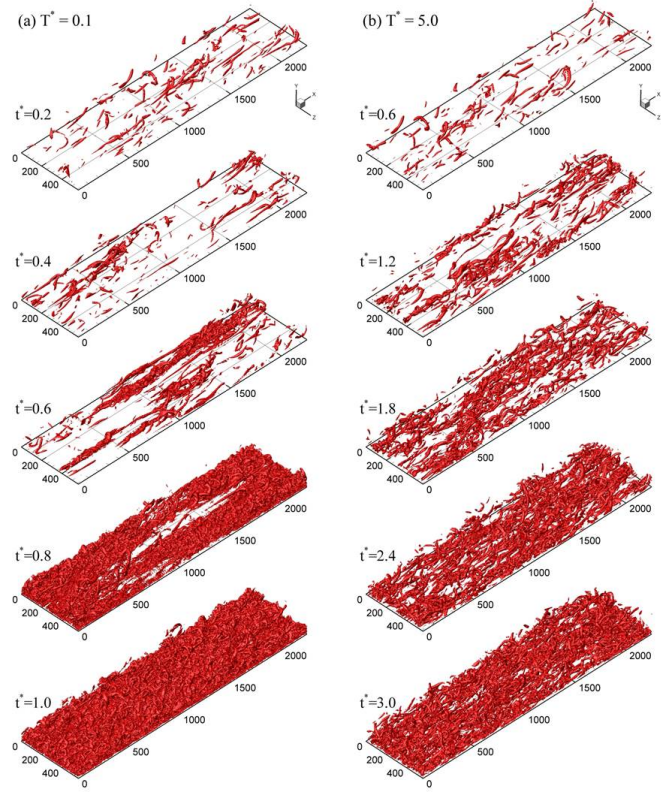


Figure 2. Instantaneous vortical structures in transient channel flows for case of $Re_{\tau,f} = 395$: (a) $T^* = 0.1$ and (b) $T^* = 5.0$. The vortices are shown as colored isosurfaces of the swirling strength for $\lambda_{ci}h/u_{\tau,i} = 30$.

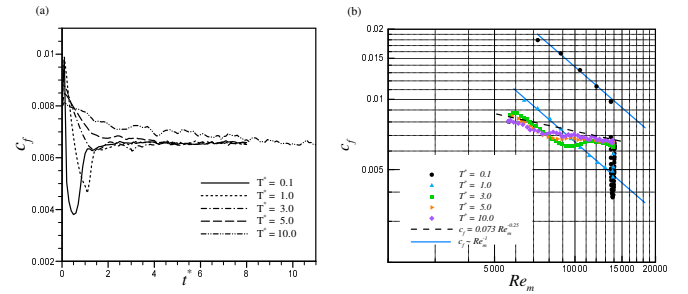


Figure 3. Development of friction coefficient with (a) non-dimensional time t^* and (b) bulk mean Reynolds number Re_m .

observed. This is because the turbulence structure is not yet fully developed, in comparison with the increased flow rate, which results in a significant difference in c_f , relative to the value in the steady state. After attaining the minimum value, c_f increases and then eventually reaches the steady state. On the other hand, when the acceleration time is long (i.e., $T^* = 5.0$ and 10.0), the value of c_f does not depart significantly from that of the steady state. In Fig. 3(b), c_f is plotted against the instant bulk Reynolds number. If the acceleration time is short (i.e., $T^* = 0.1$ and 1.0), c_f is proportional to the inverse of Re_m during the acceleration, which indicates a feature of laminar flow. This is consistent with the quasi-laminar flow, observed prior to the transition in the acceleration flow (He & Seddighi, 2013). When the acceleration time is long (i.e., $T^* = 5.0$ and 10.0), the variation in c_f with Re_m is similar to DeanFLS correlation ($c_f \sim Re_m^{-0.25}$), which implies that the turbulence structure adapts

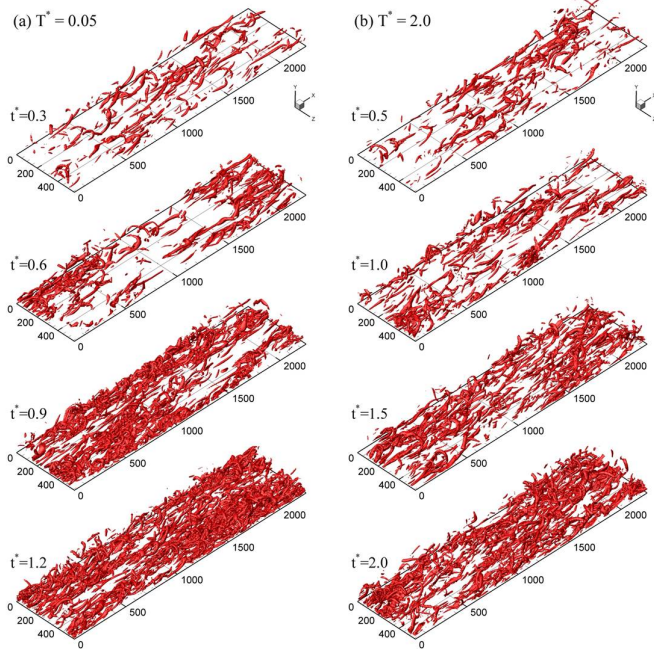


Figure 4. Instantaneous vortical structures in transient channel flows for case of $Re_{\tau,f} = 250$: (a) $T^* = 0.05$ and (b) $T^* = 2.0$. The vortices are shown as colored iso-surfaces of swirling strength for $\lambda_{c_i} h / u_{\tau,i} = 25$.

to the altered mean flow.

It has also been reported that the flow evolves progressively and the bypass-like transition process does not occur during the transient flow when the Reynolds number ratio between the final and initial stages is low (He & Seddighi, 2015). To examine the effects of the Reynolds number ratio ($Re_{\tau,f}/Re_{\tau,i}$) on the transient channel flows, four different final Reynolds numbers ($Re_{\tau,f} = 250, 300, 350,$ and 395) were tested for a fixed initial Reynolds number of $Re_{\tau,i} = 180$. Figures 4(a), and 4(b) show the changes in the vortical structures for $T^* = 0.05$ and $T^* = 2.0$ in the case of $Re_{\tau,f} = 250$, respectively. Unlike the case of $Re_{\tau,f} = 395$, even in the case where the acceleration time is short ($T^* = 0.05$), the locally clustered vortical structures are not clearly shown. However, as will be shown in Fig. 5(c), the rapid acceleration gives rise to a laminar-like flow similar to Stokes' solution at the early stage of the transient flow, which leads to a laminar-turbulent transition without involving bypass-like transition. This transient flow behavior due to a rapid acceleration for low final Reynolds number is consistent with He & Seddighi (2015).

Figure 5 shows the change in velocity distribution at the beginning of the acceleration in terms of the perturbing velocity (Figs. 5a and c) and mean velocity normalized by the friction velocity (Figs. 5b and d). The perturbation velocity is defined as (He & Seddighi, 2013, 2015):

$$\langle u \rangle^{\wedge}(y, t) = \frac{\langle u \rangle(y, t) - \langle u \rangle(y, t = 0)}{\langle u \rangle(y = h, t) - \langle u \rangle(y = h, t = 0)} \quad (4)$$

where the bracket denotes the ensemble-averaged quantity, y is the distance from the wall and t is the elapsed time after the commencement of the acceleration. He & Seddighi (2015) reported that in the case of rapid acceleration, a laminar flow similar to Stokes' first problem appears at the beginning of acceleration and then develops into a final turbulent state and this laminar-turbulent transition occurs even if the final Reynolds number is low. The present results

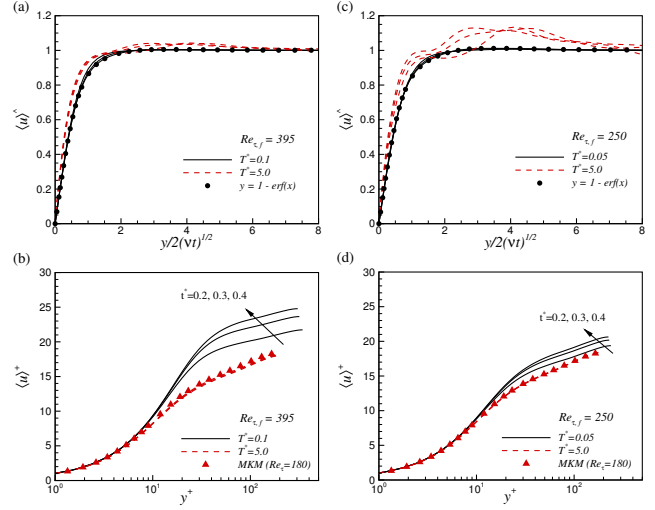


Figure 5. Development of the mean velocity profiles in the very early stage for $Re_{\tau,f} = 395$ (a, b) and $Re_{\tau,f} = 250$ (c, d). Perturbation velocity versus $y/2\sqrt{vt}$ (a, c) and mean velocity versus y^+ (b, d). Solid lines: rapid acceleration; dashed lines: slow acceleration; circles: Stokes' solution; triangles: Moser *et al.* (1999) (denoted by MKM).

also show that even for the small difference between final and initial Reynolds numbers (Fig. 5c) as well as a large difference (Fig. 5a), if the acceleration rate is high ($T^* = 0.05$ or 0.1), the change in mean velocity is very similar to the Stokes solution. As time progresses, it develops into a final turbulent flow as shown in Figs. 2(a) and 4(a). When the final Reynolds number is high, the development of the flow is similar to a bypass-like transition. On the other hand, if the final Reynolds number is low, the flow progressively evolves to the final turbulent state, which exhibits similar transient flow response characterized by the laminar-turbulent transition (He & Seddighi, 2015). It should be noted that for the very slow acceleration (denoted by red dashed lines), the perturbation velocities deviate from the Stokes solution and the mean velocities are collapsed to the profiles of the steady case even for the early stage of the acceleration, which indicates the transient flow does not undergo the laminar-turbulent transition.

Figure 6 shows the development of the maximum value of the root mean square (rms) of the fluctuating velocities normalized by the ensemble-averaged bulk mean velocity. When examining the case in which $Re_{\tau,f} = 395$ and $T^* = 0.1$ (Fig. 6a), the maximum streamwise turbulent intensity, $u'_{rms,max}$ decreases abruptly in its initial phase because the turbulence cannot react to a rapid change in the mean flow. Thereafter, it increases and reaches the final value after the overshooting (as indicated by the vertical arrow). It has also been reported that, in experiments examining pipe flow accompanied by a strong acceleration, the streamwise turbulent intensity decreases after an overshoot occurs (He & Jackson, 2000). The developments of the $v'_{rms,max}$ and $w'_{rms,max}$ are similar, but significantly different from that of $u'_{rms,max}$. The streamwise component is increased first, while the other two components denote a long delay before they increase. Such behaviors of the turbulent intensities reflect the flow characteristics of the bypass-like transition in the accelerated channel flow. The occurrence of a strong acceleration leads to a streaky structure and this structure is exposed to a secondary instability to form turbulent spots, which in turn develop into turbulent structures before reaching the final state. The generation of turbulent vortical structures promotes energy redistrib-

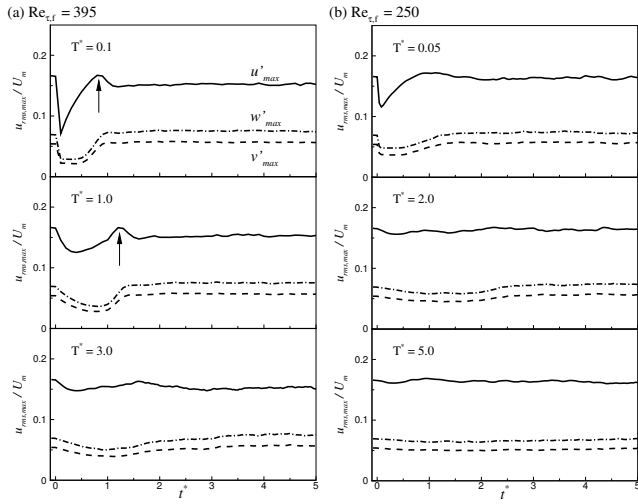


Figure 6. Development of maximum value of rms of fluctuating velocities normalized by bulk mean velocity: (a) $Re_{\tau,f} = 395$; (b) $Re_{\tau,f} = 250$.

bution (Jeong *et al.*, 1997). Thereby, the cross-stream component turbulent intensities increase, while $u'_{rms,max}$ overshoots and then decreases slightly. Since the localized peak in $u'_{rms,max}$ is associated with the enhanced streaky structure, followed by the generation of turbulent spots, the overshoot in the evolution of $u'_{rms,max}$ can be used as an indicator of the transition in the present transient channel flow. Meanwhile, for $Re_{\tau,f} = 250$ and $T^* = 0.05$ (when the acceleration rate is significant), $u'_{rms,max}$ increases after decreasing during the initial phase. However, no clear overshoot is observed. This confirms to the fact that no bypass-like transition has occurred in this case.

Figure 7(a) is a map of the occurrence of the bypass-like transition for every acceleration condition tested in the present study. The closed symbol corresponds to the bypass-like transition. If all three of the conditions below are satisfied, it is determined that a bypass-like transition has occurred.

- The laminar-like behaviors (e.g., $c_f \sim Re_m^{-1}$ and $\langle u \rangle^\wedge \approx U_{Stokes}$) are observed at the early stage of the transient flow.
- Distinct turbulent spots are generated which then develop into vortical structures in clusters.
- The overshoot in the evolution of $u'_{rms,max}$ is clearly observed.

In Fig. 7(a), when the acceleration time is long (i.e., $T^* \geq 3.0$), corresponding to a low acceleration rate, the bypass-like transition is not observed. When the ratio of the final to initial Reynolds number is small ($Re_{\tau,f} = 250$), the bypass-like transition is not clear regardless of the acceleration time. Such changes in the flow field are expected to be closely related to the amount of the impulse applied to the flow during the temporal acceleration. By integrating the pressure gradient (Eq. 3) over the acceleration period, the total impulse exerted on the flow during the acceleration can be calculated as

$$\begin{aligned}
 J^* &= \int_0^{T^*} \left(-\frac{\partial \langle p \rangle}{\partial x} \right) dt \\
 &= \underbrace{\frac{Re_m(t=T^*) - Re_m(t=0)}{2Re_{\tau,i}}}_{= \text{Increase of flow rate (A)}} + \underbrace{\int_0^{T^*} \left(\frac{Re_{\tau}^{Dean}(t)}{Re_{\tau,i}} \right)^2 dt}_{= \text{Increase of viscous friction (B)}} \quad (5)
 \end{aligned}$$

Here, J^* refers to the dimensionless total impulse which consists of

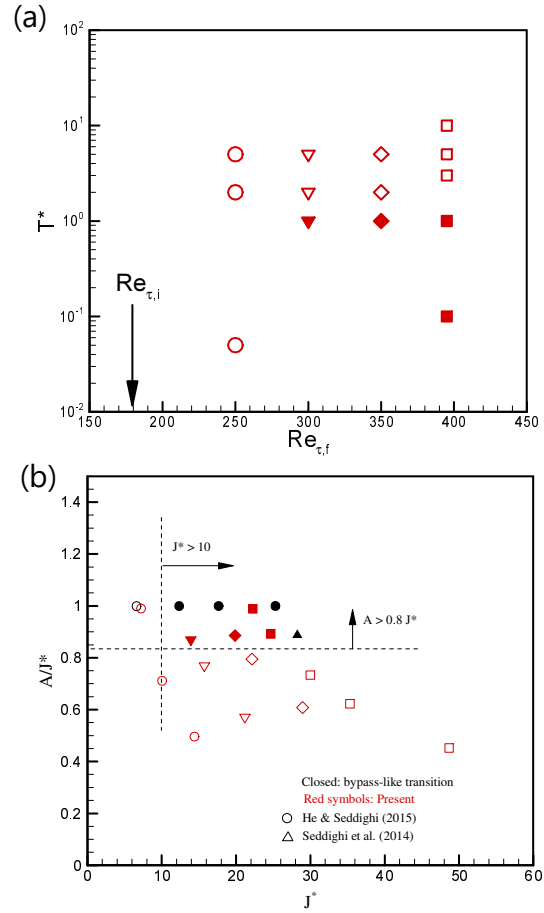


Figure 7. Conditions for transient flows similar to bypass transition due to temporal accelerations based on the (a) the final Reynolds number, $Re_{\tau,f}$ and acceleration duration, T^* and (b) the dimensionless total impulse exerted on the flow during the acceleration, J^* and its relative contribution to the increase in the flow rate, A/J^* . Red symbols denote the test cases of the present study. Closed symbols indicate the occurrence of the bypass-like transition.

the increased flow rate (A) and increased viscous friction (B). The increased flow rate (A) becomes large when the difference between the initial and final Reynolds number increases. The increased viscous friction (B) becomes more important as the acceleration time (T^*) increases. Figure 7(b) shows the relative contribution of the total impulse to the increase in the flow rate (A/J^*), relative to the total impulse applied during the acceleration. Figure 7(b) reveals that the transition in the accelerated channel flow occurs when the following conditions are satisfied:

- The total impulse exerted on the flow exceeds a critical value: $J^* > J_{cr}$.
- The relative increase in the flow rate (A) should be significant in comparison with the increased viscous friction (B). In other words, most of the total amount of impulse contributes to the increase in the flow rate: $A/J^* > c$.

The first condition is consistent with the results of the previous studies which state that the localized vortex packet is observed when the ratio of the final and initial Reynolds number is relatively high (He & Seddighi, 2015). Moreover, since J^* takes the impulse

consumed by the increased viscous friction into account, it can be explained that, in the very slow ramp-up case, the bypass-like transition is not clear even when the Reynolds number ratio is large. The second condition can be interpreted as a condition for the acceleration duration T^* . When T^* is short, the turbulence in the initial flow cannot immediately adapt to the change in the mean flow, i.e., it can be regarded as a frozen turbulence. The initial turbulence acts to the accelerated flow as a disturbance and it gives rise to a transition. In the frozen turbulence stage, Reynolds shear stress is much less than that in the non-transient flow because the turbulence does not grow yet. Because a contribution of the Reynolds shear stress to the skin friction is significant in wall-bounded flows (Fukagata *et al.*, 2002), this results in the lower increase in the wall skin friction during the flow acceleration as compared with the increase in the flow rate. On the other hand, when T^* is long, the bypass-like transition does not occur even if the Reynolds number ratio between initial and final states is high enough to cause the bypass-like transition by very rapid acceleration. In this case, the initial turbulence progressively develops according to the increase in the mean flow, which causes a significant increase in the wall skin friction relative to the increase in the flow rate. Finally, the quantitative criterion for a clear bypass-like transition in the accelerated flow, ($J^* > 10$ and $A/J^* > 0.8$), as suggested in the present study, should be identified by further studies.

CONCLUSIONS

In the present study, a detailed investigation of accelerated turbulent flows in a channel was undertaken by performing direct numerical simulations of transient turbulent flows. The simulations were started with a fully developed turbulent channel flow to which temporal accelerations were then applied. During the acceleration, nearly linear increasing excursions in the flow rate were imposed between the constant initial and final values. The initial Reynolds number based on the friction velocity was fixed at $Re_{\tau,i} = 180$ and four different final Reynolds numbers ($Re_{\tau,f} = 250, 300, 350,$ and 395) were selected to determine the effects of the Reynolds number ratio ($Re_{\tau,f}/Re_{\tau,i}$) on the transient channel flows. To elucidate the effects of the increase in the rate of the flow rates on the near-wall turbulence, we also examined a wide range of durations of acceleration.

The turbulent statistics and instantaneous flow fields revealed that a rapid increase in the flow rate invokes similar phenomena to the bypass transition in the laminar boundary layer flow, which consist of distinct turbulent spots, followed by new vortical structures, starting to appear in clusters. It has also been observed that the bypass-like transition is accompanied by the laminar-like behaviors at the early stages and the overshoot in the time evolution of the maximum streamwise turbulent intensity. In contrast, the flow evolves progressively and the transition does not occur clearly during mild flow acceleration. When the difference in the Reynolds number between the initial and final states is small during the acceleration, the bypass-like transition phenomena becomes obscure

even for a strong acceleration. The present study proposed new criteria based on the impulse applied to the flow by the temporal acceleration in order to explain the bypass-like transition to the new turbulence. This transition is mainly due to the larger contribution of the impulse to the flow rate increase compared with that to the viscous friction.

REFERENCES

- Chakraborty, P., Balachandar, S. & Adrian, R. J. 2005 On the relationships between local vortex identification schemes. *Journal of Fluid Mechanics* **535**, 189–214.
- Dean, R. B. 1978 Reynolds number dependence of skin friction and other bulk flow variables in two-dimensional rectangular duct flow. *Journal of Fluid Engineering* **100**, 215–223.
- Fukagata, K., Iwamoto, K. & Kasagi, N. 2002 Contribution of Reynolds stress distribution to the skin friction in wall-bounded flows. *Physics of Fluids* **14**, L73.
- Greenblatt, D. & Moss, E. A. 2004 Rapid temporal acceleration of a turbulent pipe flow. *Journal of Fluid Mechanics* **514**, 65–75.
- He, K., Seddighi, M. & He, S. 2016 Dns study of a pipe flow following a step increase in flow rate. *International Journal of Heat and Fluid Flow* **57**, 130–141.
- He, S. & Jackson, J. D. 2000 A study of turbulence under conditions of transient flow in a pipe. *Journal of Fluid Mechanics* **408**, 1–38.
- He, S & Seddighi, M 2013 Turbulence in transient channel flow. *Journal of Fluid Mechanics* **715**, 60–102.
- He, S & Seddighi, M 2015 Transition of transient channel flow after a change in Reynolds number. *Journal of Fluid Mechanics* **764**, 395–427.
- Jeong, J., Hussain, F., Schoppa, W. & Kim, J. 1997 Coherent structures near the wall in a turbulent channel flow. *Journal of Fluid Mechanics* **332**, 185–214.
- Jung, S. Y. & Chung, Y. M. 2012 Large-eddy simulation of accelerated turbulent flow in a circular pipe. *International Journal of Heat and Fluid Flow* **33** (1), 1–8.
- Kataoka, K., Kawabata, T. & Miki, K. 1975 The start-up response of pipe flow to a step change in flow rate. *Journal of Chemical Engineering of Japan* **8** (4), 266–271.
- Kim, K., Sung, H. J. & Adrian, R. J. 2008 Effects of background noise on generating coherent packets of hairpin vortices. *Physics of Fluids* **20**, 105107.
- Mizushima, T., Maruyama, T. & Hirasawa, H. 1975 Structure of the turbulence in pulsating pipe flows. *Journal of Chemical Engineering of Japan* **8** (3), 210–216.
- Moser, R. D., Kim, J. & Mansour, N. N. 1999 Direct numerical simulation of turbulent channel flow up to $Re_{\tau} = 590$. *Physics of Fluids* **11**, 943.
- Seddighi, M, He, S, Vardy, A. E. & Orlandi, P 2014 Direct numerical simulation of an accelerating channel flow. *Flow, Turbulence and Combustion* **92** (1-2), 473–502.